Contemporary Engineering Sciences, Vol. 13, 2020, no. 1, 263 – 291
HIKARI Ltd, www.m-hikari.com
https://doi.org/10.12988/ces.2020.91602

Efficient Technique for Solution of the 2D Buoyancy Convection Problems in Vertical Cylinders

Fedir Pletnyov and Ayodeji A. Jeje

Department of Chemical and Petroleum Engineering
Schulich School of Engineering
University of Calgary, Calgary, Alberta, Canada, T2N 1N4

Abstract

Present paper examines the two forms of the Alternating Direction Implicit (ADI) method in combination with the Polezhaev-Gryaznov (PG) vorticity boundary conditions (BC) algorithm for solving transport equations of buoyancy-induced circulation and heat transfer through Newtonian fluids in vertical cylinders. The equations were formulated in terms of the stream function, vorticity and temperature, and discretized using Central (CFD) or two forms of the Monotonic Conservative (MCFD-1 and MCFD-2) finite difference schemes of second order accuracy. The stream function equation is solved by two methods: The Fast Fourier Transform (FFT) (for grid sizes of power of 2 in vertical direction) or by Evolutionary Factorization with Logarithmic time step marching (EFL) (for arbitrary mesh sizes). The domain has rigid bottom and lateral walls with rigid or free upper surfaces. Heat enters from below; cooling is at the top and the vertical wall is insulated. The system parameters are the aspect ratio (radius/height, **a**), Rayleigh number (**Ra**) and Prandtl number (**Pr**). The effect of the convection intensity on the numerical technique efficiency was analyzed based on two cases: the weak ($Ra_{\mathrm{H}} = 2{,}500$ ($Ra_{\mathrm{R}} = 2 \cdot 10^4$)) and strong ($Ra_{\mathrm{H}} = 12{,}500$ ($Ra_{\mathrm{R}} = 10^5$)) natural convection. The Prandtl number (**Pr**) for the fluid was 7. The initial conditions for all unknowns at internal nodes were equal to zero. The choice of the vorticity BC algorithm is very important part of the numerical study. In order to clarify it four combinations of the numerical method and vorticity BC have been examined:

- ADI method (for both transient and steady state approaches) + PG vorticity BC;
- ADI method (for both transient and steady state approaches) + Woods vorticity BC;
- GS-RB (parallel) method + PG vorticity BC;
- GS-RB (parallel) method + Woods vorticity BC;

The calculations showed that for ADI method with PG algorithm for vorticity BC gives 3-8 times lower CPU time than Woods algorithm does and ADI method in both combinations of the vorticity BC works better than GS-RB (parallel) method. Also the type of the ADI method has an influence on the CPU time and solution itself in almost all conducted cases of study. The implementation of the both forms of the ADI method with steady state approach gives better results with respect to CPU time comparing to the transient approach. The parallel ADI algorithm shows higher efficiency only for finer grids (grid sizes greater or equal 129x129). The discretization of the transport equations by MCFD-1 scheme works faster in almost all simulation runs: weak and strong convection, rigid and free upper surfaces.

Keywords: ADI, Gauss-Seidel, Polezhaev-Gryaznov, boundary conditions for vorticity, monotonic conservative difference scheme, parallel algorithm, buoyancy convection, vertical cylinder, transient, steady state, efficient algorithm

Nomenclature

a	aspect ratio, R/H	σ	coefficient in convection-diffusion operator; $\sigma=1$ for $\Phi=\omega$, $\sigma=\mathrm{Pr}$ for $\Phi=\theta$
g	acceleration of gravity	ε	relative accuracy
Gr	Grashof number (= Ra/Pr)	Φ	dependent variable in the general convection-diffusion equation (θ or ω)
h_r	mesh size in the radial direction	Γ	surface of the control volume
h_z	mesh size in the axial direction	Γ^+	part of the boundary ($Nu>0$) where heat enters the fluid
H	pool height of fluid inside the cylinder	Γ^-	part of the boundary ($Nu<0$) where heat exits the fluid
L_r	radial component of convection-diffusion operator	θ	dimensionless temperature ($=\frac{T-T_c}{T_h-T_c}$)
L_z	axial component of convection-diffusion operator	ω	vorticity
N_r	number of radial mesh points	ψ	stream function

N_z	number of axial mesh points		
Nu	Nusselt number (= hR/k, h-heat transfer coeff.)	**Subscripts**	
Nu^-	Rate of heat output	c	cold
Nu^+	Rate of heat input	h	hot
Pr	Prandtl number (ν/α)	i	mesh point in r direction
r	radial coordinate	k	mesh point in z direction
R	radius of cylinder	n	iteration number
Ra_R	Rayleigh number based on radius ($\beta g \Delta T \cdot R^3 / \nu\alpha$)	r	radial component of vector
Ra_H	Rayleigh number based on height ($\beta g \Delta T \cdot H^3 / \nu\alpha$)	z	axial component of vector
T	temperature	u	uniform (function)
ΔT	temperature difference across bottom and top surfaces of domain	Ch	Chebyshev (function)
t	time	ν	kinematic viscosity
τ	time step	θ	temperature equation
υ_r	dimensionless radial component of velocity	ω	viscosity equation
υ_z	dimensionless axial component of velocity	**Superscripts**	
z	axial coordinate	+	$x^+ = \frac{1}{2}(x + \lvert x \rvert)$, x - any variable
S	number of the time steps for stream function equation	–	$x^- = \frac{1}{2}(x - \lvert x \rvert)$
f_{Ch}	Chebyshev function		
f_u	uniform function		
λ	eigen value of the Laplace operator		

1. Introduction

Many industrial systems and devices in different areas of engineering have cylindrical vertical storage tanks filled with a liquid. They may contain liquefied natural and petroleum gases, cryogenic liquids or water (solar tanks accumulating solar heat). Liquid in such types of containers is subjected to different kinds of thermal influence from ambient. Thermal load is a different combination of heating or cooling on the bottom, lateral and upper tank surfaces. As a result, natural convection inside a storage tank occurs, leading to nonuniformity of the liquid warming and high level of temperature stratification. The intensity of heat transfer

from the tank walls to liquid substantially increases and, as a result, hot light fluid floats to the upper surface. In the process of charging and withdrawal of storage tanks the degree of the vessel filling the quantity of liquid is changing, and free surface of the liquid appears. Thus, it is important to analyze of the thermal processes in storage tanks with respect to their aspect ratio (radius to height) and existence of free surface. A natural convection problem in which thin fluid layers, subjected to destabilizing temperature gradients, generates roll cells of varying forms is the Raleigh-Bernard problem: a vertical cylinder heated from below, cooled at the top and insulated on sidewall. The objective of the present work is to find a reliable and fast numerical technique to provide 2D axis-symmetric simulations of the natural convection inside vertical cylindrical tanks in an efficient way using only just simple laptop. This technique includes implementation of the combination two different forms of the ADI method, namely, classical, Peaceman and Rachford [7], ADI-PR, and evolutionary factorization, Samarskii [12], ADI-EF, along with special algorithm for estimation of the boundary conditions for vorticity. The mentioned above was developed by Polezhaev-Gryaznov [10] in 1974 for the rectangular domain, which had all rigid walls, but did not get the comprehensive use within scientists. For example, Roache [11] in his famous encyclopaedic book for computational fluid dynamics provided a very wide set of the approaches to find of the BC for vorticity. However, he did not mention the Polezhaev-Gryaznov approach. In the present paper, we extended Polezhaev-Gryaznov algorithm to cylindrical geometry, including case of the free upper surface. The results of the tests showed its significant advantage with respect to CPU time over usually employed Thom [13] and Woods [14] formulas. The only restriction we noticed from our examination is that this advantage of the Polezhaev-Gryaznov algorithm observed, when PG vorticity BC approach applied in combination with ADI method. For the stream function equation two methods are examined: Fast Fourier Transform (FFT) and Evolutionary Factorization with Logarithmic time step marching (EFL) developed by Kalitkin and Belov [3]. Mallison and de Vahl Davis [5, 6] used ADI method applying time-dependent (and thus parabolic) transport equations, and they arbitrarily included a transient term in the stream function (elliptic) equation that relate stream function and vorticity. Leong [4] has obtained 3D steady state solutions using transient approach with the ADI-EF method for transport equations in combination with FFT method for vector potential (the 3D analogue of the stream function) equations. Pletnyov and Jeje [8, 9] compared different steady state numerical methods for solution of the 2D natural convection processes in vertical cylinders such as the Gauss-Seidel Red-Black (GS-RB (parallel)) vs the Jacobian-free Newton-Krylov (JFNK), the Geometric Multigrid Method (GMG) vs the GS-RB (parallel).

In present numerical study we are comparing the technique based on the ADI method with the GS-RB (parallel) method and showing its much better efficiency. The effect of parallelization to the ADI algorithms are examined as well.

The 2D axis-symmetric algorithms for investigation of the buoyancy convection occupied a wide part of the numerical research, which require multiple runs for varying parameters, and, thus, should be efficient with respect to CPU time.

2. Problem Definition

The 2D Raleigh-Benard problem has been examined, namely, buoyancy convection in a liquid filling a vertical cylinder heated from below, cooled at the top and insulated on sidewall (Figure 1). The upper surface can be as rigid as well as flat free. The cylinder has aspect ratio $a = R / H = 2$ (R and H are the radius and height of the cylinder respectively). The critical Raleigh number based on the height , $Ra_{cr,\,\mathrm{H}}$, (onset of the convection from immobile state) according to the Charlson and Sani [1] for cylinder with aspect ratio $a = 2$ equals to 1861.27. For the Raleigh number formulated based on radius this value can be defined from the expression $Ra_{cr,\,\mathrm{R}} = a^3 \cdot Ra_{cr,\,\mathrm{H}} \approx 1.489 \cdot 10^4$. The flow pattern for the critical Raleigh number according to the Charlson and Sani [1] is axis-symmetric (two dimensional) with two rotating in opposite directions doughnut-shape rolls.

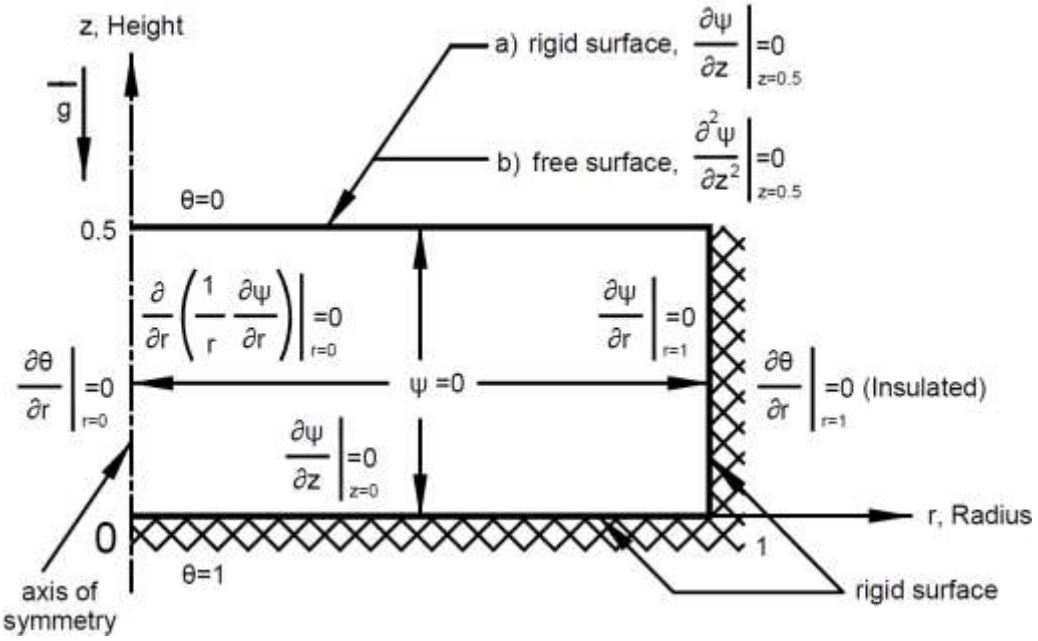

Figure 1. The 2D Raleigh-Benard problem for fluid inside the vertical cylinder with aspect ratio (radius to height) $a = 2$.

The effect of the numerical method and boundary conditions (BC) on the solution can be different for weak and strong convection. Hence, for current numerical study both cases with weak and strong convection have been considered. The Raleigh number for weak and strong convection are $Ra_{\mathrm{H}} = 2{,}500$ ($Ra_{\mathrm{R}} = 2 \cdot 10^4$) and $Ra_{\mathrm{H}} = 12{,}500$ ($Ra_{\mathrm{R}} = 10^5$) respectively. For both cases the Prandtl number $\mathrm{Pr} = 7$ (water).

3. The governing equations

The momentum vorticity and energy equations for the axisymmetric system can be written in two equivalent forms: non-conservative (non-divergent) and conservative (divergent), The choice of the form depends on the approach for finite difference discretization of the PDE. The central finite difference approximation (CFD) of the transport equations is used for the non-conservative form. CFD scheme is simple for implementation but convergence rate for strong convection is slow or algorithm even does not have convergence at all. The monotonic conservative finite difference approximation (MCFD) is used for the conservative form of the transport equations. MCFD scheme works a little bit slower for the weak convection, but much faster in case of the strong convection. Even more, MCFD scheme provides a good convergence for strong convection, when CFD scheme does not converge. The conservative form of the PDE is

$$\sum_{\alpha=1}^{2} \frac{\partial}{\partial x_\alpha} L_\alpha u + f = 0,$$

where u is the dependent variable, x_1 and x_2 are spatial coordinates, L_1 and L_2 are the convection-diffusion differential operators and f is a source function.

We will present below different forms of the transport equations in cylindrical coordinate system using the Bousinesq approximation for vorticity transport equation and after transforming from the primitive variables to vorticity-stream function ones.
The non-conservative and conservative forms of the 2D transient energy transport equation (temperature is unknown) are presented below by Eqs (1 and 1a) and Eqs (2, 2a and 2b) respectively.

$$\frac{\partial \theta}{\partial t} = \frac{1}{\mathrm{Pr}}\left(\frac{\partial^2 \theta}{\partial r^2} + \frac{1}{r}\frac{\partial \theta}{\partial r} + \frac{\partial^2 \theta}{\partial z^2}\right) - \upsilon_r \frac{\partial \theta}{\partial r} - \upsilon_z \frac{\partial \theta}{\partial z}\ , \tag{1}$$

$$r\frac{\partial \theta}{\partial t} = \frac{\partial}{\partial r}\left[r\left(\frac{1}{\mathrm{Pr}}\cdot\frac{\partial \theta}{\partial r} - \upsilon_r \theta\right)\right] + \frac{\partial}{\partial z}\left[r\left(\frac{1}{\mathrm{Pr}}\cdot\frac{\partial \theta}{\partial z} - \upsilon_z \theta\right)\right]. \tag{1a}$$

The non-conservative and conservative (two versions) forms of the 2D transient vorticity transport equations are presented below by Eqs (2, 2a and 2b) respectively.

$$\frac{\partial \omega}{\partial t} = \frac{\partial^2 \omega}{\partial r^2} + \frac{1}{r}\frac{\partial \omega}{\partial r} + \frac{\partial^2 \omega}{\partial z^2} - \frac{\omega}{r^2} + \frac{\omega \upsilon_r}{r} - \upsilon_r \frac{\partial \omega}{\partial r} - \upsilon_z \frac{\partial \omega}{\partial z} - \mathrm{Gr}\frac{\partial \theta}{\partial r}, \tag{2}$$

$$r\frac{\partial \omega}{\partial t} = \frac{\partial}{\partial r}\left[r\left(\frac{\partial \omega}{\partial r} - \upsilon_r \omega\right)\right] + \frac{\partial}{\partial z}\left[r\left(\frac{\partial \omega}{\partial z} - \upsilon_z \omega\right)\right] + \omega\left(\upsilon_r - \frac{1}{r}\right) - \mathrm{Gr}\cdot r\frac{\partial \theta}{\partial r}, \tag{2a}$$

$$\frac{\partial(r\omega)}{\partial t}=\frac{\partial}{\partial r}\left[\frac{1}{r}\cdot\left(\frac{\partial(r\omega)}{\partial r}-\upsilon_r(r\omega)\right)\right]+\frac{\partial}{\partial z}\left[\frac{1}{r}\cdot\left(\frac{\partial(r\omega)}{\partial z}-\upsilon_z(r\omega)\right)\right]-Gr\frac{\partial\theta}{\partial r}\,. \quad (2b)$$

If we apply the MCFD approximation finite difference scheme to Eq. (2a) and Eq. (2b), we will designate them as MCFD-1 and MCFD-2 respectively.

In Eqs. (1, 1a, 2, 2a and 2b) components of the velocity υ_r, υ_z and vorticity ω are defined from the expressions below as

$$\upsilon_r=-\frac{1}{r}\cdot\frac{\partial\psi}{\partial z},\ \upsilon_z=\frac{1}{r}\cdot\frac{\partial\psi}{\partial r},\ \omega=\frac{\partial\upsilon_r}{\partial z}-\frac{\partial\upsilon_z}{\partial r}.$$

The energy and vorticity transport equations have to be supplemented by stream function equation as following

$$\frac{\partial^2\psi}{\partial r^2}-\frac{1}{r}\frac{\partial\psi}{\partial r}+\frac{\partial^2\psi}{\partial z^2}=-\omega r\,. \quad (3)$$

The following dimensional quantities were used as scaling factors: for length, R the radius of cylinder, for velocity, ν/R, where ν is the kinematic viscosity of the fluid and, for temperature, $\theta=\dfrac{T-T_c}{T_h-T_c}$, where T_h and T_c are prescribed temperatures at the hot lower and cold upper surfaces. The dimensionless quantities in the equations are the Grashof (*Gr*) and Prandtl (*Pr*) numbers. Their product is the Rayleigh number (*Ra*).

We can generalize the spatial convection-diffusion differential operators in the conservative form of the transport equations (1a, 2a and 2b) as following

$$L_\alpha\Phi=\frac{\partial}{\partial\alpha}\left[a\left(\frac{1}{\sigma}\cdot\frac{\partial\Phi}{\partial\alpha}-b\Phi\right)\right]+f,\quad \alpha=r,z\,. \quad (4)$$

Eq. (1a) has the terms as

$$\Phi=\theta,\ \sigma=\mathrm{Pr},\ a=r,\ b=\upsilon_\alpha,\ f=0\,.$$

Eq. (2a) has variables and parameters defined as

$$\Phi=\omega,\ \sigma=1,\ a=r,\ b=\upsilon_\alpha,\ f=-Gr\cdot r\cdot\frac{\partial\theta}{\partial r}\ .$$

Eq. (2b) has variables and parameters defined as

$$\Phi=r\cdot\omega,\ \sigma=1,\ a=\frac{1}{r},\ b=\upsilon_\alpha,\ f=-Gr\cdot\frac{\partial\theta}{\partial r}\ .$$

4. The boundary conditions (BC)

The boundary conditions are specified as following:

1) For the stream function ψ :

a) all bounding surfaces Γ of the cylinder $z=0$, $z=\frac{1}{a}$, $r=1$ are rigid (no slip BC: $\upsilon_r\big|_\Gamma=0,\ \upsilon_z\big|_\Gamma=0$):

$$\psi\big|_\Gamma=0,\ \left.\frac{\partial\psi}{\partial n}\right|_\Gamma=0 \tag{5}$$

For stream function Eq. (3) we have overdetermination of the BC. We will employ for Eq. (3) condition $\psi\big|_\Gamma=0$ as a BC for stream function and the gradient condition $\left.\frac{\partial\psi}{\partial n}\right|_\Gamma=0$ for the determination of the BC for vorticity ω in vorticity transport equation.

b) axes of the symmetry $r=0$ ($\upsilon_r\big|_{r=0}=0,\ \left.\frac{\partial\upsilon_z}{\partial r}\right|_{r=0}=0$):

$$\psi\big|_{r=0}=0,\ \left.\frac{\partial}{\partial r}\left(\frac{1}{r}\frac{\partial\psi}{\partial r}\right)\right|_{r=0}=0 \tag{6}$$

Similar, for Eq. (3) we will use condition $\psi\big|_{r=0}=0$ for stream function on axes and condition $\left.\frac{\partial}{\partial r}\left(\frac{1}{r}\frac{\partial\psi}{\partial r}\right)\right|_{r=0}=0$ for the determination of the BC for vorticity ω in vorticity transport equation.

c) the upper surface is flat free one ($\upsilon_z=0$ and $\frac{\partial\upsilon_r}{\partial z}=0$):

$$\psi\big|_{z=\frac{1}{a}}=0,\ \left.\frac{\partial^2\psi}{\partial z^2}\right|_{z=\frac{1}{a}}=0, \tag{7}$$

The gradient condition for the stream function we will use for the vorticity BC in vorticity transport equation.

2) <u>For the vorticity</u> ω:

a) all bounding surfaces Γ of the cylinder $z=0$, $z=\frac{1}{a}$, $r=1$ are rigid (no slip BC: $\upsilon_r\big|_\Gamma=0,\ \upsilon_z\big|_\Gamma=0$):

Two conceptually different approaches we will use and compare: Woods [14] and Polezhaev-Gryaznov (PG) [10]. Both have been derived first for the rectangular coordinate system. In Woods' approach vorticity on the rigid surface can be defined by a second order approximation using values of stream function and vorticity in a single node nearest to the wall. Woods' formula requires a modification for the cylindrical coordinate system in terms of a regular mesh consisting of $N_r\times N_z$ discrete points in r and z directions respectively as following

$$\left\{\begin{array}{ll}
\left\{\begin{array}{ll}\omega_{0,k}=0, & at\ \ r=r_0=0,\\ \omega_{0,k}=\left(-\dfrac{3}{h_r^2}\psi_{1,k}-\dfrac{r_0}{2}\omega_{1,k}\right)\Big/\left(r_0+h_r\right), & at\ \ r=r_0>0,\end{array}\right.\\
\omega_{N_r-1,k}=\left(-\dfrac{3}{h_r^2}\psi_{N_r-2,k}-\dfrac{1}{2}\omega_{N_r-2,k}\right)\Big/\left(1-h_r\right), & at\quad r=1,\\
\omega_{i,0}=-\dfrac{3}{r_i h_z^2}\psi_{i,1}-\dfrac{1}{2}\omega_{i,1}, & at\ \ z=0,\\
\omega_{i,N_z-1}=-\dfrac{3}{r_i h_z^2}\psi_{i,N_z-2}-\dfrac{1}{2}\omega_{i,N_z-2}. & at\ \ z=H.
\end{array}\right. \qquad (8)$$

where $k=0,...,N_z-1$, $i=0,...,N_r-1$; h_r , h_z and N_r , N_z are respectively the mesh sizes and the number of the mesh points in r and z directions, with $\forall i,k\in\Omega/\Gamma$, where Ω/Γ are the number of internal mesh points within the domain.
The idea of the Polezhaev and Gryaznov(PG) algorithm [10] is prescription of the BC for vorticity using stream function Eq. (3) not on the border of the main domain Ω_0 but on the border of the domain Ω_1, which is one spacial step inside from the border of the main domain Ω_0 .The BC (5) for stream function is fulfilled at every single time or iteration step of the calculations.

The PG algorithm is formulated for the $n+1$ time layer as following:

1. Compute the vorticity $\omega_{i,k}^{n+1}=f(\psi_{i,k}^{n})$ by stream function Eq. (3) at the border of the smaller domain Ω_1 located one step in r and z direction inside from the border of the main Ω_0 domain as following:

$$\omega_{i,k}^{n+1}=-\frac{1}{r_i}\left[\psi_{i-1,k}^{n}\left(\frac{1}{h_r^2}+\frac{1}{2r_i h_r}\right)-2\psi_{i,k}^{n}\left(\frac{1}{h_r^2}+\frac{1}{h_z^2}\right)+\psi_{i+1,k}^{n}\left(\frac{1}{h_r^2}-\frac{1}{2r_i h_r}\right)+\frac{1}{h_z^2}\left(\psi_{i,k-1}^{n}+\psi_{i,k+1}^{n}\right)\right]; \qquad (9)$$

2. Compute $\omega_{i,k}^{n+1}$ by one of the forms for the vorticity transport equation Eqs. (2, 2a and 2b) for the inner points of the domain Ω_1 with the vorticity BC obtained in step 1.

3. Solve stream function equation for ψ_{ij}^{n+1} at the main domain Ω_0 using BC $\psi=0$ on the border of the main domain Ω_0 .

4. Adjust values for stream function on the border of the domain Ω_1 using the gradient BC for stream function $\dfrac{\partial\psi}{\partial n}=0$.

if the first order derivative is approximated by a second order forward differences (for example, in case of $i = 0$ or $k = 0$) as
$\left.\frac{\partial \psi}{\partial n}\right|_0 = -\frac{1}{2h}\left(3\psi_0 - 4\psi_1 + \psi_2\right) + O(h^2)$, then we have $\psi_0 = 0,\ \psi_1 = \frac{1}{4}\psi_2$;
if third order approximation is used for the first order derivative, then $\psi_0 = 0,\ \psi_1 = \frac{1}{2}\psi_2 - \frac{1}{9}\psi_3$. Subscripts are number of points inside the domain with ' 0 'prescribed to the border.
After that steps 1-4 are repeated until convergence.
In case of the domain with free surface, the small domain includes it.

b) axes of the symmetry $r = 0$ ($\upsilon_r\big|_{r=0} = 0,\ \left.\frac{\partial \upsilon_z}{\partial r}\right|_{r=0} = 0$):

$$\omega\big|_{r=0} = 0, \tag{10}$$

c) the upper surface is flat free one ($\upsilon_z = 0$ and $\frac{\partial \upsilon_r}{\partial z} = 0$):

$$\omega\big|_{z=\frac{1}{a}} = 0. \tag{11}$$

3) <u>for the temperature θ:</u>

$$\theta = 1 \ \ at\ \ z = 0,$$
$$\theta = 0 \ \ at\ \ z = \frac{1}{a} = 0.5, \tag{12}$$
$$\frac{\partial \theta}{\partial r} = 0 \ \ at\ \ r = 0 \ \ and\ \ r = 1.$$

5. The initial condition (guesses – for Gauss-Seidel method)

Initial guess for the transient as well as for the steady state approach is zero values for all unknowns:

$$\psi_{i,k}^0, \theta_{i,k}^0, \omega_{i,k}^0 = 0 \tag{13}$$

6. Numerical method of solution

Our goal is steady state solution of the natural convection system Eqs. (1 or 1a, 2 or 2a, 2b and 3), which can be solved by two different techniques: a) transient method for whole system by time marching until steady state is achieved; 2) steady state method, which is solved by two approaches: a) GS-RB (parallel) solves simultaneously all three equations of the system; b) every single transport equation

of the steady state system is solved in turn by ADI method using transformation steady state Eqs. (1 or 1a, 2 or 2a, 2b into parabolic equations by adding derivative of unknown (temperature or vorticity) with respect to time. Equation for stream function (3) is solved by FFT or EFL methods for both techniques.

6.1. Numerical method for solution of the transport equations

The transient equations for temperature θ Eqs. (1 and 1a) and vorticity ω Eqs. (2, 2a and 2b) we are solving and comparing by two forms of the ADI methods or GS-RB (parallel) along with stream function equation.

6.1.1. Discretization.

The discretization the transient transport equation with respect to time by Euler method can be presented in generalized form as

$$\frac{\Phi^{n+1}-\Phi^{n}}{\tau}=\Lambda_r\Phi^{n}+\Lambda_z\Phi^{n}+f^{n}\ . \tag{14}$$

Spatial approximation:

$$L_r\Phi=A_1\Phi_{i-1,k}+B_1\Phi_{i+1,k}-\left(A_1+B_1\right)\Phi_{ik}\,, \tag{15}$$

$$L_z\Phi=A_2\Phi_{i,k-1}+B_2\Phi_{i,k+1}-\left(A_2+B_2\right)\Phi_{ik}\ , \tag{16}$$

a) Central Finite Difference (CFD):

$$A_1=\frac{1}{\sigma\cdot h_r^2}+\frac{1}{2h_r}\left(\upsilon_{r,ik}-\frac{1}{\sigma\cdot r_i}\right);\ \ A_2=\frac{1}{\sigma\cdot h_z^2}+\frac{\upsilon_{z,ik}}{2h_z}; \tag{17}$$

$$B_1=\frac{1}{\sigma\cdot h_r^2}-\frac{1}{2h_r}\left(\upsilon_{r,ik}-\frac{1}{\sigma\cdot r_i}\right);\ \ B_2=\frac{1}{\sigma\cdot h_z^2}-\frac{\upsilon_{z,ik}}{2h_z}; \tag{18}$$

$$C=A_1+A_2+B_1+B_2=\frac{2}{\sigma}\left(\frac{1}{h_r^2}+\frac{1}{h_z^2}\right). \tag{19}$$

b) Monotonic Conservative Finite Difference (MCFD):

$$A_1=\frac{r_{i-\frac{1}{2}}}{h_r^3}\left[\frac{1}{1+0.5\left|\upsilon_{r\,i-\frac{1}{2},k}\right|\sigma h_r}-0.5\left(\upsilon_{r\,i-\frac{1}{2},k}-\left|\upsilon_{r\,i-\frac{1}{2},k}\right|\right)\sigma h_r\right], \tag{20}$$

$$B_1 = \frac{r_{i+\frac{1}{2}}}{h_r^3}\left[\frac{1}{1+0.5\left|\upsilon_{r\,i+\frac{1}{2},k}\right|\sigma h_r} + 0.5\left(\upsilon_{r\,i+\frac{1}{2},k} + \left|\upsilon_{r\,i+\frac{1}{2},k}\right|\right)\sigma h_r\right], \tag{21}$$

$$A_2 = \frac{r_i}{h_z^2}\left[\frac{1}{1+0.5\left|\upsilon_{z\,i,k-\frac{1}{2}}\right|\sigma h_z} - 0.5\left(\upsilon_{z\,i,k-\frac{1}{2}} - \left|\upsilon_{z\,i,k-\frac{1}{2}}\right|\right)\sigma h_z\right], \tag{22}$$

$$B_2 = \frac{r_i}{h_z^2}\left[\frac{1}{1+0.5\left|\upsilon_{z\,i,k+\frac{1}{2}}\right|\sigma h_z} + 0.5\left(\upsilon_{z\,i,k+\frac{1}{2}} + \left|\upsilon_{z\,i,k+\frac{1}{2}}\right|\right)\sigma h_z\right], \tag{23}$$

$$C = A_1 + A_2 + B_1 + B_2 . \tag{24}$$

In case of GS-RB (parallel) or SOR-RB (parallel):

$$\Phi_{ik}^{s+1} = (1-q)\Phi_{ik}^{s} + q\left(A_1\Phi_{i-1,k}^{s+1} + A_2\Phi_{i,k-1}^{s+1} + B_1\Phi_{i+1,k}^{s} + B_2\Phi_{i,k+1}^{s} + f_{ik}^{s+1}\right)/C, \tag{25}$$

where s is iteration number, q is relaxation coefficient (for GS-RB (parallel) method $q=1$).

The ADI method is absolutely stable for 2D geometry. We will use two alternative options for formulation of the ADI method: a) classical, ADI-PR, developed by Peaceman and Rachford [7]; 2) evolutionary factorization, ADI-EF, developed by Samarskii [12].

The marching from the n-th to $(n+1)$-th time layer in ADI-PR scheme is performed in two steps using intermediate time layer $n+\frac{1}{2}$ with time step $\frac{\tau}{2}$. Then Eq. (14) is substituted by two equations as

$$\begin{aligned} \frac{\Phi^{n+\frac{1}{2}} - \Phi^{n}}{\tau/2} &= \Lambda_r\Phi^{n+\frac{1}{2}} + \Lambda_z\Phi^{n} + f^{n}, \\ \frac{\Phi^{n+1} - \Phi^{n+\frac{1}{2}}}{\tau/2} &= \Lambda_r\Phi^{n+\frac{1}{2}} + \Lambda_z\Phi^{n+1} + f^{n} \end{aligned} \tag{26}$$

Both equations in (26) can be solved by the Thomas three diagonal algorithm.

After calculating values $\Phi^{n+\frac{1}{2}}$ at the intermediate time layer $n+\frac{1}{2}$, we need recalculate boundary conditions for temperature and vorticity equations, and stream function equation in case of the vorticity equation.

Evolutionary factorization form of the ADI method, ADI-EF, can be written as

$$\left(E-\frac{\tau}{2}\Lambda_r\right)\left(E-\frac{\tau}{2}\Lambda_z\right)\frac{\Phi^{n+1}-\Phi^n}{\tau}=\Lambda_r\Phi^n+\Lambda_z\Phi^n+f^n. \qquad (27)$$

Samarskii [12] proof that both form of the ADI method ADI-PR and ADI-EF are mathematically identical and have order of approximation equal to $O(\tau^2,[\max(h_r,h_z)]^2)$.

Algorithm ADI-EF is performed in three steps

1) $\left(E-\frac{\tau}{2}\Lambda_r\right)w^{(1)}=\Lambda_r\Phi^n+\Lambda_z\Phi^n+f^n$;

2) $\left(E-\frac{\tau}{2}\Lambda_z\right)w^{(2)}=w^{(1)}$;

3) $\Phi^{n+1}=\Phi^n+\tau\cdot w^{(2)}$.

This algorithm has homogeneous BC for auxiliary variables $w^{(1)}$ and , which $w^{(2)}$ does not require of the recalculating BC for Φ and stream function equation because does not have intermediate time layer. Result of application of ADI-PR and ADI-EF to temperature and vorticity equations can be different in terms of the CPU efficiency and, even, can give a different solution. The numerical results of the experiments presented below will compare both approaches.

6.2. Numerical method for solution of the stream function equation

The most efficient method tor solution of the stream function Eq. (3) is combination of the Fast Fourier Transform (FFT) in z direction and tridiagonal (Thomas) algorithm in r direction. This approach is presented in detail by Fitzpatrick [2]. The only drawback of the FFT method is restriction in cells number of discretization in z direction, namely, this number has to be power of two, i. e. 16, 32, 64, 128,.. This drawback is sometimes very important, when one wants to compare solution with the other researchers results and who use arbitrary number of the cell points or in case of the use of the Richardson extrapolation approach based on the three grid sizes. It is more efficient to apply this approach for close to each other arbitrary grid sizes. In this case another method is very challenging. This method is the ADI-EF method with set of the logarithmic time steps (EFL). This method was developed by Kalitkin and Belov [3] for Poisson equation in rectangular coordinate system. They proof that this method for Poisson equation has logarithmic convergence rate similar to FFT method. In present study we apply idea of the method to stream function Eq. (3) converting it to Poisson equation as following

$$\frac{\partial^2\psi}{\partial r^2}+\frac{\partial^2\psi}{\partial z^2}=-r\omega+\frac{1}{r}\frac{\partial\psi}{\partial r}. \qquad (28)$$

Source term of this equation is equal to $f(r,z) = -r\omega + \frac{1}{r}\frac{\partial \psi}{\partial r}$, where stream function ψ in term $\frac{1}{r}\frac{\partial \psi}{\partial r}$ we will take from previous time step. This form of the equation is essential for next calculations of the minimum and maximum eigen values of the Laplace operator, which is well known. In this case centred finite difference operators for second order derivatives are

$$\Lambda_r = \frac{\psi_{i-1,k} - 2\psi_{ik} + \psi_{i+1,k}}{h_r^2}, \quad \Lambda_z = \frac{\psi_{i,k-1} - 2\psi_{ik} + \psi_{i,k+1}}{h_z^2}. \tag{29}$$

Finite difference approximation of the right hand side (RHS) of the equation can be written as

$$f_{ik}^n = -r_i \omega_{ik} + \frac{1}{r_i}\frac{\psi_{i,k+1}^n - \psi_{i,k-1}^n}{h_r}. \tag{30}$$

Kalitkin and Belov [3] use ADI-EF method with special logarithmic set of time steps τ_s written as natural logarithm function

$$\ln(\tau_s) = 0.5\ln(\tau_{\max} \cdot \tau_{\min}) + 0.5\ln\left(\frac{\tau_{\max}}{\tau_{\min}}\right) f_s, \quad 0 \le \mathrm{s} \le \mathrm{S\text{-}1}, \tag{31}$$

where $S \approx 0.25\ln\left(\frac{\lambda_{\max}}{\lambda_{\min}}\right)\ln\left(\frac{1}{\varepsilon}\right)$ is number of the time steps $\tau_{\max}$ and $\tau_{\min}$ are maximal and minimal time steps calculated through minimum and maximum eigen values of the operators Λ_r and Λ_z as

$$\tau_{\max} = \frac{2}{\min\{\lambda_r, \lambda_z\}}; \ \tau_{\min} = \frac{2}{\max\{\lambda_r, \lambda_z\}}; \tag{32}$$

$$\min(\lambda_r) = \left(\frac{\pi}{R}\right)^2; \ \max(\lambda_r) = \left(\frac{2}{h_r}\right)^2; \tag{33}$$

$$\min(\lambda_z) = \left(\frac{\pi}{H}\right)^2; \ \max(\lambda_z) = \left(\frac{2}{h_z}\right)^2, \tag{34}$$

ε is prescribed value of the residual of the stream function equation;

$$f_s = \frac{\pi}{\pi+2} f_u + \frac{2}{\pi+2} f_{ch}, \tag{35}$$

where $f_u(s) = \frac{2s}{S}$ and $f_{ch} = \frac{\cos(\pi s)}{S+1}$ are uniform and Chebyshev functions respectively.

Our numerical experiments show that the EFL method in case of cylindrical geometry has CPU time one order worse than the FFT method but is five time better compare to the ADI-EF one with uniform time steps.

7. Estimation of Nusselt number

Nusselt number ($Nu, hR/k$) characterizes the intensity of convective heat transfer into or out of a fluid through its bounding surface Γ relative to pure conduction. This is defined as:

$$Nu = -\left.\frac{\partial\theta}{\partial n}\right|_{\Gamma}, \tag{36}$$

where θ is dimensionless temperature and variable n is the dimensionless normal to the surface Γ. Heat enters the fluid through a segment of the boundary at Γ^+ ($Nu > 0$) and exits through a different part of the boundary at Γ^- ($Nu < 0$). Here Nu describes the distribution of the dimensionless heat transfer rates over the entire bounding surface. Net heat transfer rates from the boundary into the fluid, and from the fluid to the ambient are evaluated from the integrals:

$$Nu^{+} = \frac{1}{\Gamma}\int_{\Gamma^+} Nu d\Gamma, \quad Nu^{-} = \frac{1}{\Gamma}\int_{\Gamma^-} Nu d\Gamma \tag{37}$$

For a control volume at steady state, $Nu^{+} = | Nu^{-} |$.

Since parts of the boundary Γ^+ and Γ^- may be unknown in advance, it is convenient to estimate Nusselt numbers for input and output heat rates by integrating over the native boundary Γ from the following relationships:

$$\begin{aligned} Nu^{+} &= \frac{1}{2\Gamma}\int_{\Gamma}\left(Nu + |Nu|\right)d\Gamma, \\ Nu^{-} &= \frac{1}{2\Gamma}\int_{\Gamma}\left(Nu - |Nu|\right)d\Gamma. \end{aligned} \tag{38}$$

The total heat rate through the bounding surfaces is as

$$Nu = \frac{1}{2}\left(Nu^{+} + \left|Nu^{-}\right|\right). \tag{39}$$

Since Leong [4] used the height of the cylinder, H, for non-dimensionalizing and defined it per unit area, the Nusselt number (Nu_L) in the paper is related to value in equation (39) as

$$Nu_L = \frac{Nu}{a}, \tag{40}$$

where $a = R/H$ is aspect ratio.

8. Criteria for convergence

a) Relative errors for the dependent variables, from consecutive iterations, are specified as:

$$\max(\varepsilon_\theta, \varepsilon_\omega, \varepsilon_\psi) < \varepsilon, \tag{41}$$

$$\varepsilon_{\xi} = \max\left|\varepsilon_{i,\mathrm{j}}^{(\xi)}\right|; \quad \varepsilon_{i,\mathrm{j}}^{(\xi)} = \frac{1}{\bar{\xi}^{s}}\left(\xi_{i,\mathrm{j}}^{s+1} - \xi_{i,\mathrm{j}}^{s}\right),$$

where

$$\bar{\xi}^{s} = \sum_{i,\mathrm{j}} \frac{\left|\xi_{i,\mathrm{j}}^{s}\right|}{N_r \cdot N_z}; \quad \xi = \theta, \omega, \psi;$$

$N_r \cdot N_z$ is the total number of the points in grid, n is the iteration number; ε is tolerance for relative error, $\varepsilon \approx 10^{-3} - 10^{-8}$.

b) Maximum value of the residual (defect) in the Eqs. (1, 1a, 2, 2a, 2b and 3) from all points of the domain:

$$d_{\max,\xi} = \max\left|d_{i,\mathrm{j}}^{(\xi)}\right| < \varepsilon_1, \quad \xi = \omega, \theta, \psi \,. \tag{42}$$

Here ε_1 is tolerance for maximum value of the defect $\varepsilon_1 \approx 0.1 - 10^{3}$.

c) Average value of the residual in the Eqs. (1, 1a, 2, 2a, 2b and 3) from all points of the domain.

$$d_{aver,\xi} = \sum_{i,\mathrm{j}} \frac{\left|d_{i,\mathrm{j}}\right|}{N_r \cdot N_z} < \varepsilon_2; \quad \xi = \theta, \omega, \psi; \tag{43}$$

d) Convergence and balance of the heat transfer (Nusselt number) from the bottom to the top of the cylinder

$$\frac{\left|\tilde{N}u_{n+1}^{+} - \tilde{N}u_{n}^{+}\right|}{\tilde{N}u_{n+1}^{+}} \le \varepsilon_3 \,. \tag{44}$$

9. Results and discussion

Following presented an examination of the simulation results of the 2D natural convection of the fluid inside the vertical cylindrical storage tank varying forms of the transport equations, algorithms for vorticity BC, types of the upper surface (rigid and free) as well as the characteristics of the computational approach (sequential or parallel). The Rayleigh - Benard problem, where bottom surface is heated, upper surface is cooled and sidewall is insulated, has been chosen for examination. The particular parameters of the problem were following: aspect ratio $a = R/H = 2$, Prandtl number $\mathrm{Pr} = 7$, Raleigh number $Ra_{\mathrm{H}} = 2{,}500$ ($Ra_{\mathrm{R}} = 2 \cdot 10^{4}$) and $Ra_{\mathrm{H}} = 12{,}500$ ($Ra_{\mathrm{R}} = 10^{5}$) for weak and strong convection respectively. Two numerical methods for solution of the natural convection system, namely, ADI and GS-RB have been used and compared in present numerical study. Solutions of the simulation shown in Figures 2 and 3. Solutions are not unique. For the case of weak convection $Ra_{\mathrm{H}} = 2500$ ($Ra_{\mathrm{R}} = 2 \cdot 10^{4}$) we observed flow pattern with two rotating in opposite direction circular rolls for rigid upper surface. Let us designate solution as “Solution 2-2” , where first digit “2” means number of rolls, the second digit “2” (after dash) means direction of the rotation along the axes of the cylinder (“1”: in clockwise

direction, "2" : in counter clockwise direction). Solution 2-1 is possible as well, but another initial condition/guess should be used for temperature (see Pletnyov and Jeje [9]). In case of the free upper surface four different solutions have been obtained: with one and two rotating in opposite direction rolls. Different solutions can be obtained manipulating the used numerical method (ADI or GS-RB) and BC algorithm for vorticity. The grid size has been chosen identical for all depicted in Figures 2 and 3 simulations: $65(r)\times 65(z)$. In case of the free surface the intensity of the convection is $\sim (25-40)\%$ higher compare to rigid upper surface (compare Nusselt number Nu in Figures 2 and 3). In case of strong convection two solutions "Solution 1-1" (one roll) and "Solution 2-1" (two rolls) have been observed for rigid upper surface. Both solutions have clockwise direction of the rotation near the axes of the cylinder. In case of the free surface flow pattern with only one roll for two solutions (rotation in opposite directions) "Solution 1-1" and "Solution 1-2" have been found. Nusselt number for strong convection is much higher compare to weak convection: rigid upper surface 2.36 vs 1.24 and for free surface 2.88 vs 1.75.

9.1. Effect of the BC for vorticity method on the CPU efficiency

Table 1 (rigid upper surface) and Table 2 (free upper surface) describe the CPU efficiency, number of the iterations along with Nusselt number for the simulation of the weak ($Ra_H = 2{,}500$ ($\mathrm{Ra}_R = 2\cdot 10^4$) and strong ($Ra_H = 12{,}500$ ($\mathrm{Ra}_R = 10^5$) convections with respect to BC for vorticity method.

The ADI-PR method with MCFD-1 approximation has been chosen for the comparison of the transient and steady state approaches. The ratio CPU time for vorticity BC by Woods to CPU time by Polezhaev-Gryaznov demonstrate how much faster the PG approach is compare to the Woods approach. It is 3- 6 times faster only if ADI method is used both for transient and steady state methods, for GS-RB and SOR (parallel) methods both BC approaches are almost equal. The best results with respect to CPU time demonstrates implementation of the ADI method for steady state solution of the natural convection system, when transport equations are solved in turn. If we comparing PG approach for two steady state methods: ADI and GS-RB (parallel) methods, we can conclude that the efficiency of the ADI method is 5-15 times better. Combination of the PG approach with BC for vorticity with ADI method for solution of the transport equations is the best choice with respect to PU time for solution 2D non-linear natural convection system in cylindrical coordinates.

Figure 3 shows the convergence rate of the Nusselt number to reach steady state solution with respect to the iterations of time for PG and Woods approaches. The case of study is the strong convection, $Ra_H = 12{,}500$ ($\mathrm{Ra}_R = 10^5$), rigid upper surface. The ADI-PR method has been employed as for transient as well as for steady state technique. As can be seeing, PG approach requires 2-5 times fewer iterations compare to Woods' approach. As a result, the required CPU time is reduced as well. The cases with free surface and weak convection demonstrate very similar behaviour.

9.2. Effect the implemented ADI method forms for transient and steady state methods on the CPU efficiency.

As we mentioned in section 6.1, there are two possible formulations of ADI method, namely, ADI-PR and ADI-EF. Application of those formulations to temperature and vorticity equations can give different efficiency and, even, different solution. In Tables 3 (rigid upper surface) and 4 (free upper surface) are presented a comparison (CPU time, number of the iteration, Nusselt number) of the use different forms of the ADI methods (PR and EF) implemented for transient and steady state approaches for weak and strong convection with respect to different type of finite different approximation (MCFD-1, MCFD-2, CFD). The BC for vorticity is Polezhaev-Gryaznov (PG), grid size is 65x65. The stream function equation is solved by FFT method. In case of the rigid upper surface the fastest performance to get "Solution 2-2" in case of weak convection demonstrates CFD approximation with ADI-EF method applied both for temperature and vorticity equations. A little bit worse result gives MCFD-1 approximation. "Solution 1-2" obtained using MCFD-2 approximation along with ADI-EF for temperature and ADI-PR for vorticity equations. For the case of strong convection, $Ra_H = 12,500$ ($\mathrm{Ra}_R = 10^5$), the best results give the MCFD-1 approximation in combination with ADI-EF method applied for temperature and vorticity equations. "Solution 1-1" is obtained only using steady state method with just different time step for vorticity equations compare the "Solution 2-2". Thus, time step can influence on solution as well.

In case of the free upper surface three different solutions: "Solution 1-1", "Solution 1-2" and "Solution 2-2" have been obtained for weak convection and two different solutions: "Solution 1-1"and "Solution 1-2" for strong convection.

For weak convection, fastest way to get "Solution 1-2" is use ADI-EF method for both temperature and vorticity equations along with MCFD-1 approximation. For "Solution 1-1" the fastest CPU performance gives ADI-EF for both temperature and vorticity equations along with CFD approximation. The only way to obtain "Solution 2-2" is use of the ADI-PR method for both transport equations along with CFD approximation. For strong convection the fastest way to get "Solution 1-1" and "Solution 1-2" is usage of the MCFD-1 approximation. Application of the ADI-PR method for both transport equations gives the fastest way to obtain "Solution 1-1" and ADI-EF method for temperature equation and ADI-PR method for vorticity equation using steady state approach to get "Solution 1-2". In general, the MCFD-1 approximation demonstrates the fastest way to get solution for both cases of rigid and free surfaces for both weak and strong convection.

9.3. Effect the different mesh sizes on the solution and the CPU efficiency.

Table 5 describes comparison of the CPU time for the Rayleigh -Benard problem using ADI-PR, ADI-EF and GS-RB (parallel) methods (steady state approach) with respect to grid size. The rigid upper surface was considered and for approximation of the transport equations the MCFD-1 finite difference scheme has been used. The time steps τ_θ and τ_ω for temperature and vorticity equations have been chosen as optimal to get the fastest CPU performance.

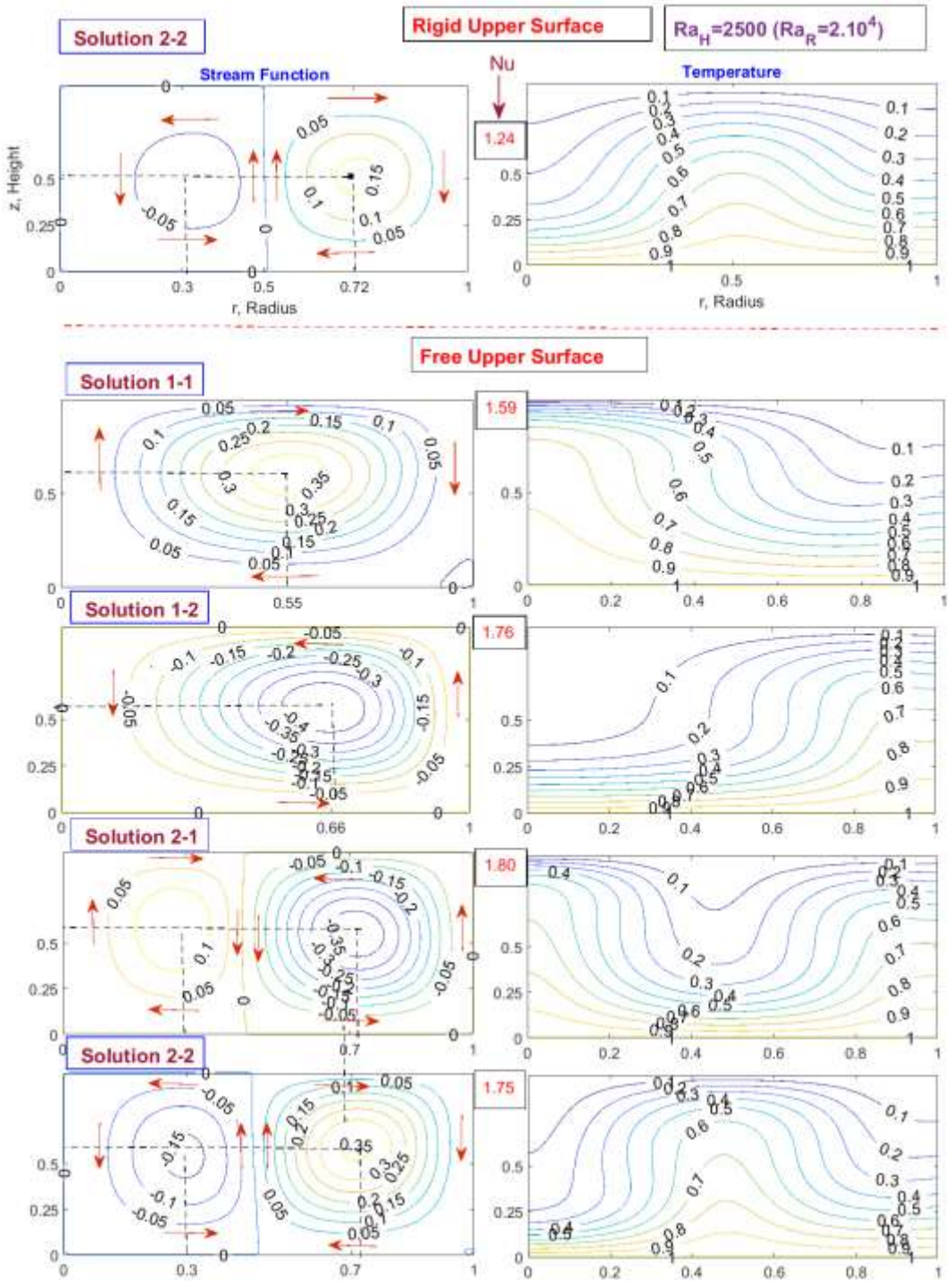

Figure 2. The solutions of the Rayleigh -Benard problem. Axis-symmetrical case: $Ra_H = 2{,}500$ $(\mathrm{Ra}_R = 2 \cdot 10^4)$, $\mathrm{Pr} = 7$, $a = R / H = 2$

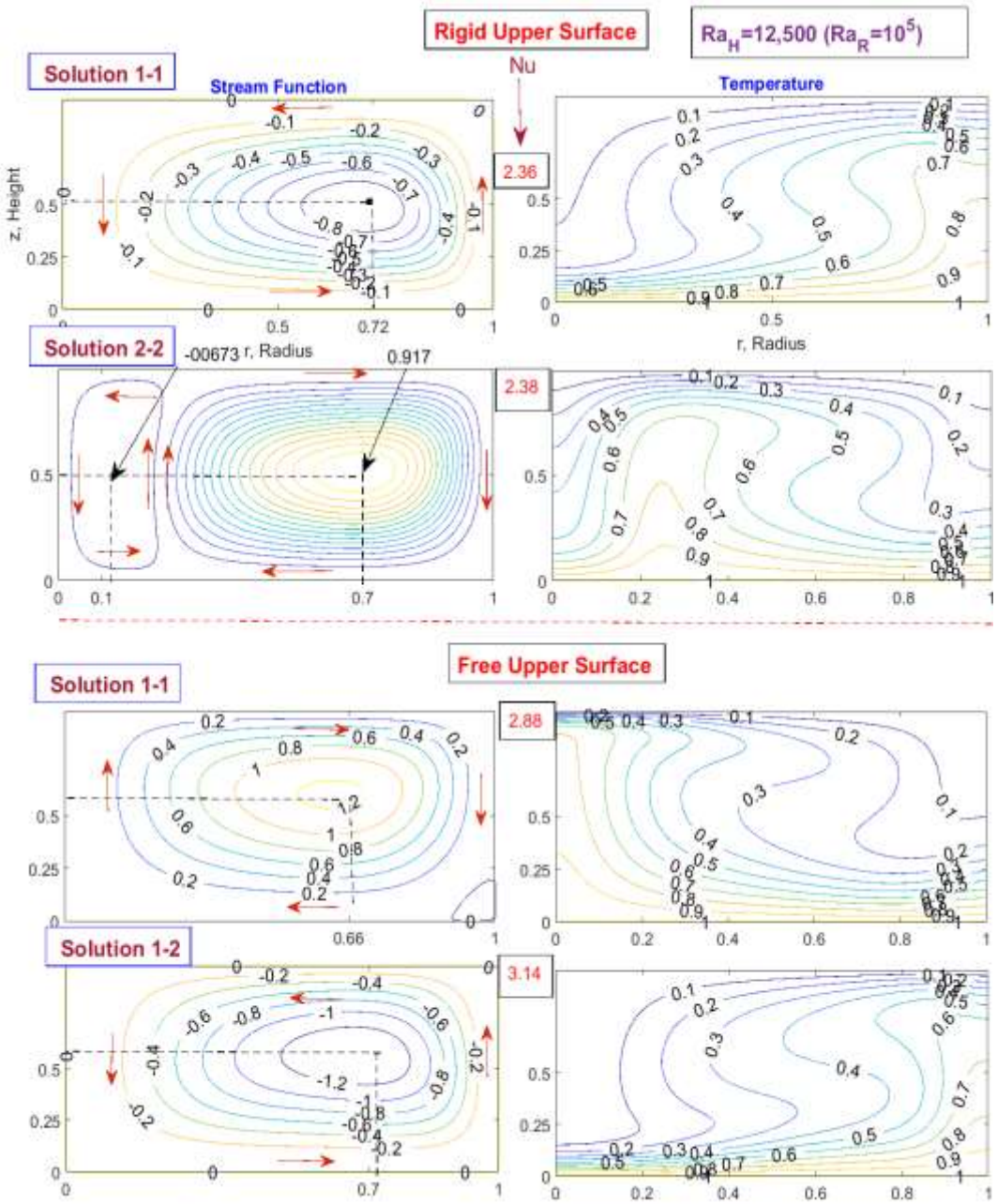

Figure 3. The solutions of the Rayleigh -Benard problem. Axis-symmetrical case: $Ra_H = 12{,}500$ ($\mathrm{Ra}_R = 10^5$), $\mathrm{Pr} = 7$, $a = R/H = 2$

The use of the different types of the ADI methods can give different solutions. In case of the ADI-EF type, different solutions are able possible by manipulating the time steps for the temperature and vorticity equations. For example, in case of the grid size 33x33, the solutions "Solution 2-2" and " Solution 1-2" were obtained using the same time step for vorticity equation $\tau_\omega = 1.4 \cdot 10^{-3}$ and two different time

steps for temperature equation $\tau_\theta = 1.5 \cdot 10^{-2}$ and $\tau_\theta = 2 \cdot 10^{-3}$ respectively; for grid sizes 65x65 and 129x129 tree different solution solutions: "Solution 1-1", "Solution 1-2" and "Solution 2-2" have been obtained varying time steps for both transport equations. The best CPU time for obtaining "Solution 2-2" shows the use of the ADI-EF method for temperature equation and ADI-PR method for the vorticity equation for the grid sizes 33x33 and 129x129 and ADI-PR method for both transport equations for grid size 65x65. The results for GS-RB (parallel) is presented as well for comparison. For all presented grid sizes ADI methods demonstrates 5-7 times better the CPU time compare to the GS-RB (parallel) method. Relative accuracy for whole system was $\varepsilon = 10^{-6}$. For solution every single transport equation the relative accuracy was $\varepsilon_\theta, \varepsilon_\omega = 10^{-1}$ (Not high). This option gives the best convergence rate for the system.

9.4. Effect the parallelization of the ADI method on the CPU efficiency.
Table 6 describes comparison of the parallel and sequential implementations of the BC for vorticity by Polezhaev-Gryaznov [10] algorithm with respect to grid size and for rigid and free upper surfaces. The transient ADI-PR method and case of the strong convection, $Ra_H = 12,500$ ($\mathrm{Ra}_R = 10^5$) were chosen for current analysis. CPU time has been measured on the same machine using Intel processor i7-3970X, 3.5 GHz, 6 cores. For parallel algorithms Task Parallel Library (TPL) of the Microsoft Visual Studio and C# computer language were used. Parallel algorithm requires additional overhead expenses for calculations and, hence, make sense to use it only for very finer grids. In our case, for rigid upper surface it is 129x129 and greater, and for free surface it is 257x257 and greater.

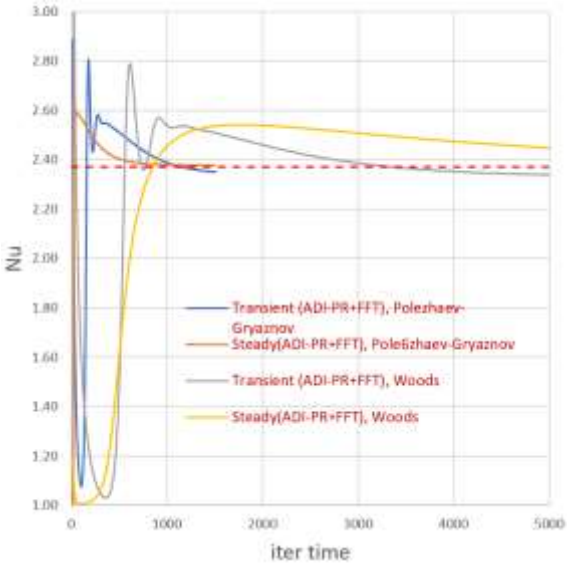

Figure 4. Convergence of the Nusselt number Nu to "Solution-2" using BC for vorticity by Polezhaev-Gryaznov[] and Woods[] by transient and steady state ADI-PR+FFT methods; $Ra_H = 12,500$ ($\mathrm{Ra}_R = 10^5$), $\mathrm{Pr} = 7$, $a = R/H = 2$.

Table. 1. Effect of the BC for vorticity method on the CPU efficiency of the simulation for weak and strong convections; grid size 65x65; transport equations approximated by MCFD-1 scheme; rigid upper surface.

Ra_H=2,500 (Ra_R=2*10^4) -weak convecti		MCFD-1				Sol 2-2	Rigid Upper Surface		
Numerical Method	BC	q_ω	τ	τ_Θ	τ_ω	CPU, s	CPU_Woods/ CPU_PG	iter	Nu
Transient	PG	1	2.4*10^{-4}	-	-	11.82		2,268	1.22
(ADI-PR+FFT)	Woods	1	7.5*10^{-5}	-	-	45.93	3.89	11,157	1.22
Steady state	PG	1	-	10^{-3}	2.3*10^{-4}	7.17		2,268	1.24
(ADI-PR+FFT)	Woods	1	-	10^{-3}	7.7*10^{-5}	22.62	3.15	5,001	1.24
Transient	PG	1	2.3*10^{-4}	-	-	59.09		3,764	1.22
(ADI-PR+EFL)	Woods	1	7.1*10^{-5}	-	-	341.97	5.79	11,544	1.22
Steady state	PG	1	-	10^{-3}	2.3*10^{-4}	38.17		2,266	1.24
(ADI-PR+EFL)	Woods	1	-	10^{-3}	7.1*10^{-5}	137.99	3.62	4914	1.24
Steady state	PG	1	-	-	-	35.46		25,559	1.24
(GS-RB_paral.)	Woods	1	-	-	-	36.28	1.02	25,242	1.24
Steady state	PG	1.6	-	-	-	-		-	-
(SOR-parallel)	Woods		-	-	-	28.67		20,921	1.24
Ra_H=12,500 (Ra_R=10^5) - strong convection									
Numerical Method	BC	q_ω	τ	τ_Θ	τ_ω	CPU, s	CPU_Woods/ CPU_PG	iter	Nu
Transient	PG	1	2.4*10^{-4}	-	-	11.13		3,825	2.34
(ADI-PR+FFT)	Woods	1	7.5*10^{-5}	-	-	36.61	3.29	10,077	2.33
Steady state	PG	1	-	10^{-3}	2.3*10^{-4}	7.98		2,228	2.38
(ADI-PR+FFT)	Woods	1	-	10^{-3}	7.710^{-5}	22.55	2.83	4,794	2.37
Transient	PG	1	2.3*10^{-4}	-	-	53.34		3,936	2.34
(ADI-PR+EFL)	Woods	1	7.1*10^{-5}	-	-	276.48	5.18	11,204	2.34
Steady state	PG	1	-	10^{-3}	2.3*10^{-4}	35.91		2,311	2.38
(ADI-PR+EFL)	Woods	1	-	10^{-3}	7.1*10^{-5}	156.15	4.35	5254	2.38
Steady state	PG	1	-	-	-	31.73		22,933	2.38
(GS-RB_paral.)	Woods	1	-	-	-	29.72	0.94	23,069	2.37
Steady state	PG	1.6	-	-	-	-		-	-
(SOR-parallel)	Woods		-	-	-	23.37		17,847	2.37

‘PG -Polezhaev-Gryaznov

‘yellow highlight – the fastest run

Table. 2. Effect of the BC for vorticity on the CPU efficiency of the simulation for weak and strong convections; grid size 65x65; transport equations approximated by MCFD-1 scheme; free upper surface.

Ra_H=2,500 (Ra_R=2*10^4) -weak convecti						MCFD-1 Sol 1-1	Free Upper Surface		
Numerical Method	BC	q_ω	τ	τ_Θ	τ_ω	CPU, s	CPU_Woods/ CPU_PG	iter	Nu
Transient	PG	1	2.4*10^{-4}	-	-	13.97		4,790	1.57
(ADI-PR+FFT)	Woods	1	7.5*10^{-5}	-	-	62.11	4.45	15,194	1.52
Steady state	PG	1	-	10^{-3}	2.4*10^{-4}	9.77		2,882	1.59
(ADI-PR+FFT)	Woods	1	-	10^{-3}	7.8*10^{-5}	34.36	3.52	7,467	1.54
Transient	PG	1	2.4*10^{-4}	-	-	72.81		4,760	1.57
(ADI-PR+EFL)	Woods	1	7.1*10^{-5}	-	-	443.60	6.09	15,640	1.53
Steady state	PG	1	-	10^{-3}	2.4*10^{-4}	48.44		2,880	1.59
(ADI-PR+EFL)	Woods	1	-	10^{-3}	7*10^{-5}	225.87	4.66	47646	1.55
Steady	PG	1	-	-	-	123.64		33,985	1.55
(GS-RB_paral.)	Woods	1	-	-	-	120.18	0.97	33,985	1.55
Steady state	PG	1.6	-	-	-	-		-	-
(SOR-parallel)	Woods		-	-	-	96.74		26,733	1.55
Ra_H=12,500 (Ra_R=10^5) - strong convection									
Numerical Method	BC	q_ω	τ	τ_Θ	τ_ω	CPU, s	CPU_Woods/ CPU_PG	iter	Nu
Transient	PG	1	2.4*10^{-4}	-	-	4.48		1,406	2.88
(ADI-PR+FFT)	Woods	1	7.8*10^{-5}	-	-	14.99	3.35	3,909	2.84
Steady state	PG	1	-	10^{-3}	2.3*10^{-4}	2.86		616	2.88
(ADI-PR+FFT)	Woods	1	-	10^{-3}	7.7*10^{-5}	8.36	2.92	1,457	2.84
Transient	PG	1	2.4*10^{-4}	-	-	20.77		1,406	2.88
(ADI-PR+EFL)	Woods	1	7.1*10^{-5}	-	-	110.37	5.31	4,260	2.85
Steady state	PG	1	-	10^{-3}	2.3*10^{-4}	13.05		618	2.88
(ADI-PR+EFL)	Woods	1	-	10^{-3}	7.1*10^{-5}	54.12	4.15	1,588	2.85
Steady state	PG	1	-	-	-	-		-	-
(GS-RB_paral.)	Woods	1	-	-	-	30.36		8,434	2.85
Steady state	PG	1.6	-	-	-	-		-	-
(SOR-parallel)	Woods		-	-	-	25.40		6,963	2.85

‘PG -Polezhaev-Gryaznov

‘Tr. -Transient method; St. – Steady state method;

‘yellow highlight – the fastest run

Table. 3. Effect the ADI method form implemented for transient and steady state methods for weak and strong convection with respect to different type of finite different approximation (MCFD-1, MCFD-2, CFD); BC for vorticity by Polezhaev-Gryaznov (PG); grid size 65x64; rigid upper surface.

Method: ADI+FFT | BC for ω by PG | **Rigid Upper Surface**

Ra_H=2,500 (Ra_R=$2*10^4$) -weak convection | 65x65 | Pr=7 | a=R/H=2

ADI type		τ	τ_Θ	τ_ω	CPU, s		iter		Nu		Solution		Rolls
Θ	ω	Transient	Steady State		Tr.	St.	Tr.	St.	Tr.	St.	Tr.	St.	
MCFD-1													
PR	PR	$2.4*10^{-4}$	10^{-3}	$2.3*10^{-4}$	11.82	7.17	3,768	2,268	1.22	1.24	2-2		2
PR	EF	$3.1*10^{-4}$	10^{-3}	$3*10^{-4}$	10.82	7.27	3,358	2,374	1.22	1.24	2-2		2
EF	EF	$3.1*10^{-4}$	10^{-1}	$2.3*10^{-4}$	23.15	5.18	7,513	1,569	1.22	1.24	2-2		2
EF	PR	$2.3*10^{-4}$	10^{-1}	$3*10^{-4}$	27.19	7.06	8,994	2,290	1.22	1.24	2-2		2
MCFD-2													
PR	PR	$7.6*10^{-5}$	10^{-3}	$4.4*10^{-5}$	27.67	14.26	9,552	4,936	1.22	1.24	2-2		2
PR	EF	$7.6*10^{-5}$	10^{-3}	$4*10^{-5}$	29.82	18.08	9,552	5,404	1.22	1.24	2-2		2
EF	EF	$7.6*10^{-5}$	10^{-1}	$4.4*10^{-5}$	68.96	10.88	22,878	3,436	1.22	1.24	2-2		2
EF	PR	$7.6*10^{-5}$	10^{-1}	$4*10^{-5}$	67.52	12.56	22,878	4,070	1.22	1.24	1-2		1
CFD													
PR	PR	$2.3*10^{-4}$	$8*10^{-3}$	$2.3*10^{-4}$	52.31	7.55	18,019	2,134	1.22	1.25	2-2		2
PR	EF	$2.3*10^{-4}$	$8*10^{-3}$	$2.3*10^{-4}$	54.24	7.88	18,019	2,128	1.22	1.25	2-2		2
EF	EF	$2.3*10^{-4}$	10^{-1}	$2.3*10^{-4}$	53.21	4.58	18,019	1,164	1.22	1.25	2-2		2
EF	PR	$2.3*10^{-4}$	10^{-1}	$2*10^{-4}$	51.19	5.00	18,019	1,465	1.22	1.25	2-2		2

Ra_H=12,500 (Ra_R=10^5) - strong convection

ADI type		τ	τ_Θ	τ_ω	CPU, s		iter		Nu		Solution		Rolls
Θ	ω	Transient	Steady State		Tr.	St.	Tr.	St.	Tr.	St.	Tr.	St.	
MCFD-1													
PR	PR	$2.3*10^{-4}$	10^{-3}	$2.3*10^{-4}$	11.66	7.32	3,825	2,228	2.34	2.38	2-2		2
PR	EF	$3.1*10^{-4}$	10^{-3}	$3.1*10^{-4}$	16.29	14.72	5257	4,775	2.34	2.38	2-2		2
EF	EF	$3.1*10^{-4}$	10^{-1}	$3.1*10^{-4}$	5.94	6.02	1,627	1,522	2.32	2.36	1-1		1
		-	10^{-3}	$3.1*10^{-4}$	-	3.44	-	953	-	2.36	1-2		1
		-	10^{-3}	$2.3*10^{-4}$	-	14.67	-	4,912	-	2.38	2-2		2
EF	PR	$2.3*10^{-4}$	10^{-3}	$2.3*10^{-4}$	6.34	2.47	2,032	569	2.32	2.36	1-2		1
MCFD-2													
PR	PR	$7.5*10^{-5}$	10^{-3}	$4*10^{-5}$	22.62	9.38	7,703	3,038	2.34	2.43	2-2		2
PR	EF	$7.5*10^{-5}$	10^{-3}	$4*10^{-5}$	22.77	10.08	7,703	3,038	2.34	2.43	2-2		2
EF	EF	$7.6*10^{-5}$	10^{-1}	$4*10^{-5}$	16.71	4.43	5,446	1,245	2.32	2.37	1-1		1
EF	PR	$7.6*10^{-5}$	10^{-1}	$4*10^{-5}$	16.62	4.24	5,446	1,245	2.32	2.37	1-1		1
CFD													
PR	PR	$2.3*10^{-4}$	$9*10^{-3}$	$2.3*10^{-4}$	73.19	16.20	25,677	5,213	2.33	2.37	2-2		2
PR	EF	$2.3*10^{-4}$	$9*10^{-3}$	$2.3*10^{-4}$	77.11	16.65	25,676	5,211	2.33	2.37	2-2		2
EF	EF	$2.3*10^{-4}$	10^{-1}	$2.3*10^{-4}$	74.30	14.05	25,676	4,174	2.33	2.37	2-2		2
EF	PR	$2.3*10^{-4}$	10^{-1}	$2*10^{-4}$	75.34	13.75	25,677	4,177	2.33	2.37	2-2		2

Table. 4. Effect the ADI method form implemented for transient and steady state methods for weak and strong convection with respect to different type of finite different approximation (MCFD-1, MCFD-2, CFD); BC for vorticity by Polezhaev-Gryaznov (PG); grid size 65x64; free upper surface upper surface.

Method: ADI+FFT						BC for ω by PG				Free Upper Surface			
Ra_H=2,500 (Ra_R=2*10^4) -weak convection						65x65				Pr=7 a=R/H=2			
ADI type		τ	τ_Θ	τ_ω	CPU, s		iter		Nu		Solution		Rolls
Θ	ω	Transient	Steady State		Tr.	St.	Tr.	St.	Tr.	St.	Tr.	St.	
MCFD-1													
PR	PR	2.4*10^{-4}	10^{-3}	2.4*10^{-4}	14.40	9.26	4,790	2,882	1.57	1.59	1-1		1
PR	EF	3.2*10^{-4}	10^{-3}	3*10^{-4}	10.49	7.27	3,513	2,803	1.61	1.63	1-1		1
EF	EF	3.2*10^{-4}	10^{-1}	3*10^{-4}	6.43	7.49	2,010	2,342	1.76	1.63	1-2	1-1	1
EF	PR	2.4*10^{-4}	10^{-1}	2.3*10^{-4}	9.78	5.62	3,344	1,608	1.70	1.59	1-2	1-1	1
MCFD-2													
PR	PR	7.7*10^{-5}	10^{-3}	4.5*10^{-5}	43.14	33.65	14,700	11,552	1.53	1.60	1-1		1
PR	EF	7.7*10^{-5}	10^{-3}	4.5*10^{-5}	46.24	13.66	15,910	4,338	1.52	1.77	1-1	1-2	1
EF	EF	7.7*10^{-5}	10^{-1}	4.5*10^{-5}	31.30	32.49	9,668	11,404	1.65	1.60	1-2	1-1	1
EF	PR	7.7*10^{-5}	10^{-1}	4.5*10^{-5}	29.69	13.73	9,519	4,070	1.66	1.24	1-2	1-1	1
CFD													
PR	PR	2.4*10^{-4}	8*10^{-3}	2.4*10^{-4}	88.56	13.82	28,951	4,398	1.75	1.77	2-2		2
PR	PR	-	9*10^{-3}	2.4*10^{-4}	-	6.05	-	1,770	-	1.80	-	2-1	2
PR	EF	2.4*10^{-4}	8*10^{-3}	2.4*10^{-4}	73.50	9.29	23,780	2,806	1.62	1.63	1-1		1
PR	EF	-	9*10^{-3}	2.4*10^{-4}	-	7.10	-	2,165	-	1.76	-	2-1	2
EF	EF	2.4*10^{-4}	10^{-1}	2.4*10^{-4}	73.82	5.48	23,780	1,508	1.62	1.63	1-1		1
EF	PR	2.4*10^{-4}	10^{-1}	2.4*10^{-4}	89.06	7.15	28,951	2,013	1.75	1.61	2-2	1-1	2, 1
Ra_H=12,500 (Ra_R=10^5) - strong convection													
ADI type		τ	τ_Θ	τ_ω	CPU, s		iter		Nu		Solution		Rolls
Θ	ω	Transient	Steady State		Tr.	St.	Tr.	St.	Tr.	St.	Tr.	St.	
MCFD-1													
PR	PR	2.4*10^{-4}	10^{-3}	2.3*10^{-4}	4.61	2.48	1,406	615	2.88	2.88	1-1		1
PR	EF	3.2*10^{-4}	10^{-3}	3.2*10^{-4}	5.46	5.06	1,696	1,317	2.92	2.91	1-1		1
EF	EF	3.2*10^{-4}	1.6*10^{-3}	2.6*10^{-4}	4.60	6.89	1,379	1,578	3.17	2.91	1-2	1-1	1
EF	EF	-	1.6*10^{-3}	2.7*10^{-4}	-	3.96	-	1,149	-	3.22	-	1-2	1
EF	PR	2.4*10^{-4}	10^{-3}	2.3*10^{-4}	4.47	1.98	1,404	429	3.12	3.16	1-1	1-2	1
EF	PR	-	10^{-1}	2.3*10^{-4}	-	5.25	-	1,545	-	2.88	-	1-1	1
MCFD-2													
PR	PR	7.7*10^{-5}	10^{-3}	4.4*10^{-5}	11.66	6.10	3,609	1,627	2.84	2.89	1-1		1
PR	EF	7.7*10^{-5}	10^{-3}	4.4*10^{-5}	11.39	6.29	3,621	1,673	2.83	2.89	1-1		1
EF	EF	7.7*10^{-5}	10^{-1}	4.4*10^{-5}	11.48	4.93	3,590	1,245	3.10	2.89	1-2	1-1	1
EF	PR	7.7*10^{-5}	10^{-1}	4.4*10^{-5}	11.70	4.96	3,584	1,209	3.11	2.89	1-2	1-1	1
CFD													
PR	PR	2.4*10^{-4}	8*10^{-3}	2.4*10^{-4}	20.15	4.20	6,456	1,023	2.92	2.92	1-1		1
PR	EF	2.4*10^{-4}	8*10^{-3}	2.4*10^{-4}	20.03	3.80	6,410	920	2.94	2.93	1-1		1
EF	EF	2.4*10^{-4}	10^{-1}	2.4*10^{-4}	19.94	3.37	6,410	704	2.92	2.37	1-1		1
EF	PR	2.4*10^{-4}	10^{-1}	2.4*10^{-4}	20.02	3.60	25,677	809	2.92	2.37	1-1		1

Table 5. Comparison of the CPU time for the Rayleigh -Benard problem using ADI-PR, ADI-EF and GS-RB (parallel) methods (steady state approach) with respect to grid size. $Ra_H = 12{,}500$ ($\mathrm{Ra}_R = 10^5$), $\mathrm{Pr} = 7$, $a = R/H = 2$ .rigid upper surface, approximation by MCFD-1 finite difference scheme.

ADI type		33x33					65x65				
Θ	ω	τ_T	τ_W	Nu	CPU s	Sol.	τ_T	τ_W	Nu	CPU s	Sol.
PR	PR	$5*10^{-3}$	10^{-3}	2.4	1.18	2-2	10^{-3}	$2.3*10^{-4}$	2.38	7.32	2-2
PR	EF	$5*10^{-3}$	$1.3*10^{-3}$	2.4	1.59	2-2	10^{-3}	$3.1*10^{-4}$	2.38	14.72	2-2
EF	EF	$1.5*10^{-2}$	$1.4*10^{-3}$	2.4	1.54	2-2	10^{-1}	$3.1*10^{-4}$	2.36	6.02	1-1
		$2*10^{-3}$	$1.4*10^{-3}$	2.38	0.77	1-2	10^{-3}	$3.1*10^{-4}$	2.36	3.44	1-2
		-	-	-	-	-	10^{-3}	$2.3*10^{-4}$	2.38	14.67	2-2
EF	PR	$2*10^{-2}$	10^{-3}	2.4	1.09	2-2	10^{-3}	$2.3*10^{-4}$	2.36	2.47	1-2
GS-RB (paral)		-	-	2.4	6.5	2-2	-	-	2.38	32.7	2-2

Table 5. (cont.)

ADI type		129x129				
Θ	ω	τ_Θ	τ_ω	Nu	CPU s	Sol.
PR	PR	$2.5*10^{-4}$	$2*10^{-5}$	2.4	226.23	2-2
PR	EF	$2.5*10^{-4}$	$7*10^{-5}$	2.4	255.8	2-2
EF	EF	$5*10^{-4}$	$7*10^{-5}$	2.4	56.51	1-2
		$5*10^{-2}$	$7*10^{-5}$	2.4	69.58	1-1
		$5*10^{-2}$	$5*10^{-5}$	2.4	296.7	2-2
EF	PR	$5*10^{-2}$	$5*10^{-5}$	2.4	90.59	2-2
GS-RB (paral)		-	-	2.4	393.4	2-2

Table 6. Comparison of the parallel vs sequential implementations of the BC for vorticity by Polezhaev-Gryaznov [] with respect to grid size and for rigid and free upper surfaces; Transient ADI-PR method; $Ra_H = 12,500$ ($\mathrm{Ra}_R = 10^5$) .

rigid upper surface

Grid size	τ	CPU, s		CPU par./ CPU seq.	iter	Nu
		seq.	paral			
17x17	6.00E-03	0.59	0.71	0.83	317	2.32
33x33	1.00E-03	1.33	1.55	0.86	1,076	2.33
65x65	2.30E-04	10.86	10.96	0.99	3,825	2.34
129x129	5.50E-05	176.30	167.38	1.05	13,785	2.34
257x257	1.00E-05	2961.48	2,298.10	1.29	60,874	2.35

free upper surface

Grid size	τ	CPU, s		CPU par./ CPU seq.	iter	Nu
		seq.	paral			
17x17	9.00E-03	0.69	0.80	0.86	772	2.98
33x33	1.00E-03	0.77	0.84	0.92	351	2.95
65x65	2.40E-04	4.40	4.64	0.95	1,417	2.89
129x129	5.00E-05	72.43	73.80	0.98	6,237	2.87
257x257	1.00E-05	1,333.60	1,062.23	1.26	27,536	2.87

10. Conclusion

The effect of application the boundary conditions (BC) for vorticity developed by Polezhaev-Gryaznov [10] and Woods [14] on the convergence rate of the Alternating Direction Implicit (ADI) and Gauss-Seidel Red-Black (GS-RB (parallel)) methods was investigated. Two forms of the ADI method were examined: ADI-PR (Peaceman and Rachford [7]) and ADI-EF (evolutionary factorization, Samarskii [12]).

The problem investigated was the steady natural convection of a fluid confined within a closed vertical cylinder of the aspect ratio (radius to height) $a = R / H = 2$, with heating at the bottom, cooling at the top and insulated sidewall. Both rigid and free upper surfaces were considered. Two types of discretization were used: central (CFD) and two forms of the monotonic conservative (MCFD-1 and MCFD-2). For the problem formulated in terms of stream function, vorticity and temperature, the initial values of the temperature, stream function and vorticity at interior nodes were set at zero. Two different types of the steady natural convection intensities were studied, weak ($Ra_H = 2,500$ ($\mathrm{Ra}_R = 2 \cdot 10^4$) and strong

($Ra_H = 12,500$ ($\mathrm{Ra}_R = 10^5$) . The Prandtl number was kept constant at 7. The results are presented as stream function contours for circulation patterns, isotherms for temperature profiles, solution name and Nusselt numbers that correlate to the heat transfer rates.

The effect of the technique for vorticity BC is significant in combination with the ADI method (for both transient and steady state approaches) and almost identical in combination with the GS-RB (parallel) method. For the ADI method CPU time was 3-10 times lower when Polezhaev-Gryaznov approach was used compared to the application of the Woods approach. The type of the ADI method was influence on the CPU time and solution itself for almost all simulations. The fastest performance demonstrated the use of the ADI-EF method for both temperature and vorticity equations. The use of the both forms of the ADI method with steady state approach gave better results with respect to CPU time.

The parallel ADI algorithm shown higher efficiency only for finer grids (grid sizes greater than 129x129). The discretization by MCFD-1 worked faster in almost all cases of study: weak and strong convection, rigid and free upper surfaces.

References

[1] Charlson G. S. and Sani R. L., Thermal Instability in a Bounded cylinder Fluid Layer, *Int. J. Heat Mass Transfer*, **13** (1970), 1479-1496. https://doi.org/10.1016/0017-9310(70)90181-x

[2] R. Fitzpatrick, *Computational Physics: An Introduction Course*, 2014, http://farside.ph.utexas.edu/teaching/329/lectures/lectures.html

[3] N. N. Kalitkin and A. A. Belov, Analogue of the Richardson Method for Logarithmically Converging Time Marching, *Doclady Mathematics*, **452** (3) (2013), 261-265.

[4] M. S. S. Leong, Numerical study of Rayleigh-Benard convection in a cylinder, *Numerical Heat Transfer, Part A*, **41** (2002), 673-683. https://doi.org/10.1080/104077802317418287

[5] G. D. Mallinson and G. de Vahl Davis, Three-dimensional convection in a box: a numerical study, *J. Fluid Mech.*, **83** (1977), 1-31. https://doi.org/10.1017/s0022112077001013

[6] G. D. Mallinson and G. de Vahl Davis, The Method of the False Transient for the solution of Coupled Elliptic Equations, *J. Comput. Phys.*, **12** (1973), 435-461. https://doi.org/10.1016/0021-9991(73)90097-1

[7] D. W. Peaceman and H. H. Rachford, The numerical solution of parabolic and elliptic differential equations, *J. Soc. Indust. Appl. Math.*, **3** (1955), 28-41. https://doi.org/10.1137/0103003

[8] F. Pletnyov and A. Jeje, Geometric Multigrid Method for Steady Buoyancy Convection in Vertical Cylinders, *Contemporary Engineering Sciences*, **9** (2) (2016), 47-70. https://doi.org/10.12988/ces.2016.511306

[9] F. Pletnyov and A. Jeje, The Gauss-Seidel (GS) and the Jacobian-Free Newton-Krylov (JFNK) Methods Applied to Steady 2D Buoyancy Convection in Vertical Cylinders, *Contemporary Engineering Sciences*, **12** (4) (2019), 187-228. https://doi.org/10.12988/ces.2019.9828

[10] V. I. Polezhaev and V. L Gryaznov, Method of calculating the boundary conditions for the Navier–Stokes equations in the "vorticity, stream function" variables, *Dokl. Akad. Nauk SSSR*, **219** (2) (1974), 301–304. (in Russian)

[11] P. J. Roache, *Fundamentals of Computational Fluid Dynamics*, Hermosa Publishers Albuquerque, New Mexico, USA, 1998.

[12] A. A. Samarskii, *The Theory of Difference Schemes*, Marcel Dekker Inc., 2001, pp. 543-553. https://doi.org/10.1201/9780203908518

[13] Thom A., The flow past circular cylinders at low speeds, *Proc. Roy. Soc, London A*, **141** (1933), 651-669. https://doi.org/10.1098/rspa.1933.0146

[14] L. C. Woods, A note on the numerical solution of fourth order differential equations, *Aeronautical Quarterly*, **5** (1954), 176-184. https://doi.org/10.1017/s0001925900001177

Received: October 7, 2020; Published: October 25, 2020